

Experimental Characterization of the Optical Loss of Sapphire-Bonded Photonic Crystal Laser Cavities

M. H. Shih, Wan Kuang, Tian Yang, Mahmood Bagheri, Zhi-Jian Wei, Sang-Jun Choi, Ling Lu, John D. O'Brien, *Senior Member, IEEE*, and P. Daniel Dapkus, *Fellow, IEEE*

Abstract—Sapphire-bonded photonic crystal laser cavities with varying number of photonic crystal periods were studied in order to determine the optical loss in these cavities. The lasing threshold increases as the number of lattice periods decreases, and the quality factors of these cavities were calculated from the lasing threshold data. Continuous-wave operation was achieved for cavities with eight or more cladding periods.

Index Terms—Continuous-wave (CW) lasers, microcavity, optical losses, photonic crystal, quality factors, semiconductor lasers.

TWO-DIMENSIONAL (2-D) photonic crystal lasers have interesting potential as light sources in dense chip-scale optical systems. Many designs of the photonic crystal laser cavities have been demonstrated [1]–[6], but there are a limited number of reports of room-temperature continuous-wave (CW) operation [4], [7]. In this letter, we report on a method to determine the optical losses in 2-D sapphire-bonded photonic crystal laser cavities by varying the number of photonic crystal periods cladding the defect resonant cavity. This work was done with photonic crystal resonant cavities formed in InGaAsP membranes bonded to a sapphire ($\alpha\text{-Al}_2\text{O}_3$) substrate. This substrate functions both as a heat sink and as a low refractive index cladding layer [8]. With a sufficient number of lattice periods cladding the cavity, these devices are capable of room-temperature CW operation. While the analysis is performed here for a photonic crystal cavity on a sapphire substrate, the method can be applied generally to photonic crystal lasers.

These devices were fabricated in a 240-nm-thick InGaAsP layer, containing four InGaAsP strained quantum wells designed to emit near $1.55\ \mu\text{m}$ at room temperature, on an InP substrate that was deposited by metal–organic chemical vapor deposition. The InGaAsP wafer was then bonded to a 240- μm -thick sapphire substrate, and annealed in a H_2 chamber at $505\ ^\circ\text{C}$. A mask consisting of a silicon nitride layer and 3% polymethylmethacrylate resist was then deposited on the sample. The photonic crystal cavities were defined using electron beam lithography, and the photonic crystal patterns were transferred into the InGaAsP layers using a reactive ion etch and electron cyclotron resonance dry etching steps. The

Manuscript received June 9, 2005; revised November 15, 2005. This study is based on research supported by the Defense Advanced Research Projects Agency (DARPA) under Contract F49620-02-1-0403 and by the National Science Foundation under Grant ECS-0094020.

The authors are with the Department of Electrical Engineering–Electrophysics, University of Southern California, Los Angeles, CA 90089 USA (e-mail: minhsius@usc.edu).

Digital Object Identifier 10.1109/LPT.2005.863993

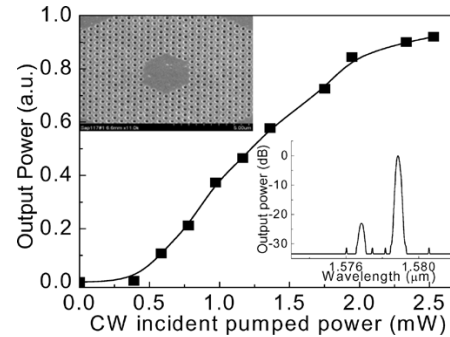


Fig. 1. The L – L curve of a photonic laser cavity under CW optical pumping condition. The inset image is an SEM image of this 37 missing hole cavity with 11 periods of lattice cladding. The lasing spectrum is also shown in the bottom inset.

details of the fabrication have been discussed in a previous work [7].

The photonic crystal laser cavities were formed in a region in which 37 holes were missing (D4 cavity) from a 2-D triangular photonic crystal lattice. These cavities are approximately $3.2\ \mu\text{m}$ in diameter. In this study, we fabricated a series of photonic crystal laser devices in which the number of photonic crystal periods cladding the cavity varied between 3 and 8 periods. Cavities with 11 periods were also fabricated on the same sample. All of the laser cavities were optically pumped at room temperature using an 850-nm diode laser at normal incidence. The pump spot was focused by a $100\times$ objective lens to a spot about $2.5\ \mu\text{m}$ in diameter. The output power was collected by a multimode fiber connected to an optical spectrum analyzer.

Fig. 1 shows the CW output power versus input power lasing data of a D4 laser cavity with 11 periods of photonic crystal. The left inset image is a scanning electron microscope (SEM) image of this D4 photonic crystal laser cavity, and the right inset is a plot of the lasing spectrum in logarithm scale. This data was taken at room temperature. The lasing wavelength is $1579\ \text{nm}$ and its threshold occurred with 0.4-mW incident optical power.

To evaluate the optical loss of these sapphire-bonded photonic crystal cavities, we measured the threshold characteristics of the set of devices in which number of photonic crystal periods cladding the cavity varied between three and eight periods. Fig. 2 shows an SEM image of the array. The two inserts show magnified images of cavities with three and seven periods of photonic crystal cladding, respectively. The input power versus output power (L – L) curves from the four typical cavities with five to eight periods of cladding are shown in Fig. 3. Lasing was not achieved in cavities with less than five periods of photonic

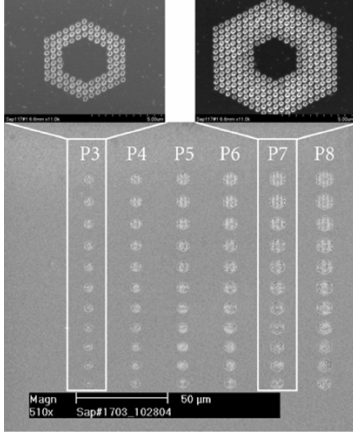


Fig. 2. SEM image of the sapphire-bonded photonic crystal laser array. The number of photonic crystal periods is varied from three (P3) to eight (P8), and the lattice constant of a cavity is varied from 360 to 460 nm in each column. The two insets are images of two elements in the array with three and seven periods of photonic crystal cladding, respectively.

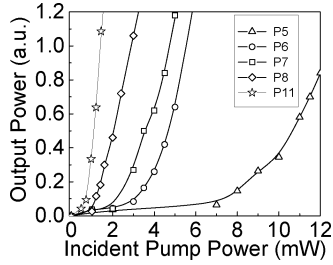


Fig. 3. Incident pump power versus output power ($L-L$) curves from five photonic crystal laser cavities with 5–11 periods of photonic crystal cladding.

crystal cladding. All five laser cavities had the same lattice constant, 400 nm, and were optically pumped at room temperature with a 1% duty cycle and an 8-ns pulse width. In addition, all devices are lasing in the same mode at 1579 nm and had a typical sidemode suppression ratio of about 15 dB under these pulsed conditions. As shown in Fig. 3, the incident threshold pump power of these cavities increases from 0.95 to 7 mW as the number of cladding periods decreases from eight to five as expected. The slope of these $L-L$ curves generally decreases as the number of photonic crystal periods decreases, also as expected. The quality (Q) factors of these photonic crystal cavities were estimated from the threshold pump power of each cavity using a simple model. The incident optical power was converted into an effective current (I_{elec}) and the recombination currents due to radiative (I_{sp}), Auger (I_{auger}), and surface recombination (I_{sr}) were determined using the coefficients in [9]. Then the modal gain can be determined for a quantum-well laser using [10]

$$G = G_0 \ln \left(\frac{I_{\text{elec}} - I_{\text{sr}}}{I_{\text{tr}}} \right) \quad (1)$$

where G_0 is the modal gain coefficient of 68.4 cm^{-1} for our photonic crystal lasers and I_{tr} is the transparency current for our quantum well. G_0 was determined from material gain measurements made on broad area lasers with the same active region as in [10] and then the confinement factor was calculated from

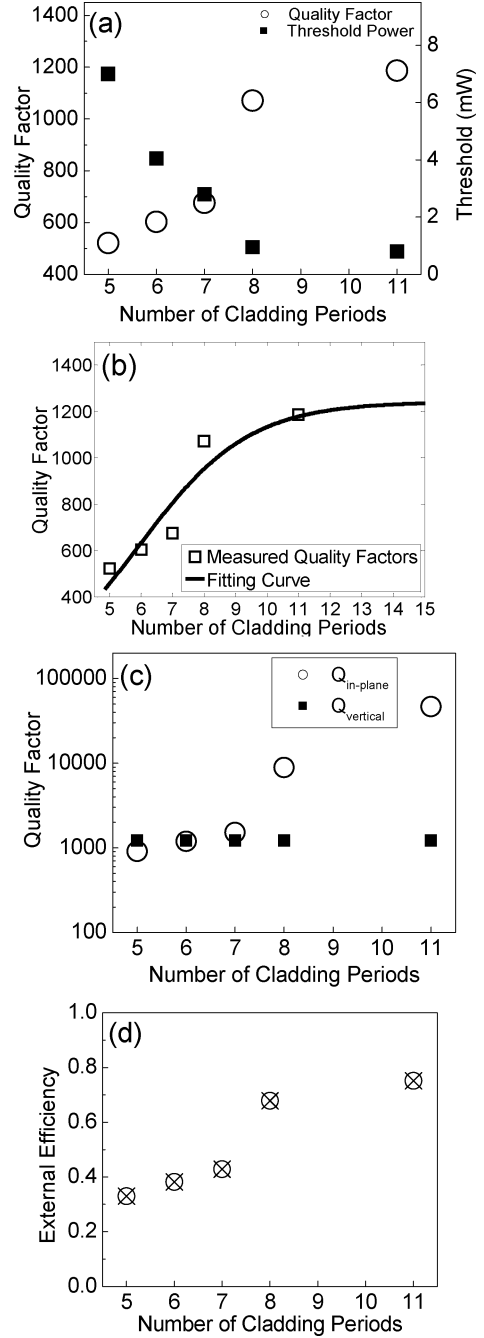


Fig. 4. (a) Quality factors and threshold power versus the number of photonic crystal cladding periods. (b) Total quality factors of the photonic crystal cavities. The square-dots are the extracted total quality factors and the solid-line is the fitting curve for the data. (c) in-plane and vertical quality factors extracted from the data in Fig. 4(a). (d) External efficiency of the cavities with different number of photonic crystal cladding periods.

a simple finite difference algorithm. The quality factors of the cavities were obtained from the threshold modal gains using

$$Q = \frac{2\pi n_{\text{InP}}}{\lambda G_{\text{th}}} \quad (2)$$

where $n_{\text{InP}} = 3.17$ and G_{th} is the threshold modal gain.

Fig. 4(a) shows the extracted quality factors (hollow circles) and the incident threshold power (solid squares) versus the number of photonic crystal periods. At eight periods, we obtain

a Q value of 1100, and in a device with 11 periods we obtained a Q of 1200. This data agrees very well with a three-dimensional finite-difference time-domain calculation that predicts a theoretical quality factor of 1200 for this mode in a cavity in this geometry with eight cladding periods. This calculated Q is limited by radiation loss into the sapphire substrate.

The varying optical loss across the array allows the extraction of the in-plane and out-of-plane radiation loss components in these cavities as well. Using the threshold pump power data and a simple model, we fit the in-plane and out-of-plane quality factors as a function of the number of cladding periods. The total quality factor contains the in-plane and the out-of-plane quality factors

$$\frac{1}{Q_{\text{total}}} = \frac{1}{Q_{\text{in-plane}}} + \frac{1}{Q_{\text{out-of-plane}}}. \quad (3)$$

The in-plane quality factor depends on the reflectivity of the photonic crystal periods cladding the cavity. Based on the results of coupled mode theory of distributed Bragg reflectors [11], we model $Q_{\text{in-plane}}$ as

$$\frac{1}{Q_{\text{in-plane}}} = b \ln \left(\frac{1}{R} \right) \quad (4)$$

$$R = \tanh^2(c\tau_l) \quad (5)$$

where R is the reflectivity, τ_l is the number of cladding periods, and b and c are the fitting constants. Since the out-of-plane radiation loss depends on the in-plane cavity geometry and the cavity thickness, which did not change across the array of devices, we modeled the out-of-plane Q as a constant. The fitting result of the total quality factors is shown in Fig. 4(b). The square points are the extracted total quality factors of the cavities, and the solid line is the fitting curve using (3)–(5). We obtained an out-of-plane quality factor of these photonic crystal cavities of just over 1200. The in-plane and out-of-plane quality factors as a function of the number of cladding periods are shown in Fig. 4(c). This data shows strong similarities to numerical models of these components of the quality factors calculated for smaller cavities [12], [13]. Once the in-plane and out-of-plane components of the quality factor have been determined, we can also estimate the slope efficiency that might be achieved in these cavities from

$$\eta_{\text{ext}} \approx \frac{1}{\frac{Q_{\text{vertical}}}{1}} \times \frac{n_{\text{sap}}^3}{n_{\text{sap}}^3 + 1} \times T_{\text{sap}} \times \eta_{\text{in}}. \quad (6)$$

This relation is for the slope efficiency as seen from the sapphire side of these cavities. Here the ratio of the indexes of refraction accounts for the different coupling into the sapphire and air sides of these cavities, T_{sap} is the modal transmittivity of the sapphire interface, and η_{in} is the internal efficiency. This relation is for the slope efficiency as seen from the sapphire side

of the cavities. Here the ratio of the indexes of refraction accounts for the different coupling into the sapphire and air sides of these cavities. Fig. 4(d) shows the ratio of the inverse of the out-of-plane quality factor to the inverse of the total quality factor multiplied by the ratio of indexes of refraction ratio as a function of cladding periods. This plot represents the expected slope efficiency that might be obtained from these devices for unity internal efficiency and unity transmission through the sapphire interface. On this sample, CW lasing of the cavities was observed in the devices with either 8 or 11 periods of photonic crystal cladding the cavity. The cavities with five, six, and seven cladding periods can only be operated under pulsed condition. This result implies the minimum cladding periods for our CW laser is eight.

In summary, we observed that the threshold power of laser cavities increased with decreasing number of photonic crystal periods cladding a laser cavity. The quality factors of these photonic crystal cavities were extracted using this data. We also observed the CW operation of the cavities with eight more cladding periods of photonic crystal.

REFERENCES

- [1] J. D. O'Brien, O. Painter, R. Lee, C. C. Cheng, A. Yariv, and A. Scherer, "Laser incorporating 2D photonic bandgap mirrors," *Electron. Lett.*, vol. 32, pp. 2243–2244, 1996.
- [2] O. Painter, R. K. Lee, A. Scherer, A. Yariv, J. D. O'Brien, P. D. Dapkus, and I. Kim, "Two-dimensional photonic bandgap defect mode laser," *Science*, vol. 284, pp. 1819–1821, 1999.
- [3] M. Imada, S. Noda, A. Chutinan, T. Tokuda, M. Murata, and G. Sasaki, "Coherent two-dimensional lasing action in surface-emitting laser with triangular-lattice photonic crystal structure," *Appl. Phys. Lett.*, vol. 75, pp. 316–8, 1999.
- [4] J. K. Hwang, H. Y. Ryu, D. S. Song, I. Y. Han, H. K. Park, D. H. Jang, and Y. H. Lee, "Continuous room-temperature operation of optically pumped two-dimensional photonic crystal lasers at 1.6 μm ," *IEEE Photon. Technol. Lett.*, vol. 12, no. 10, pp. 1295–1297, Oct. 2000.
- [5] H. Y. Ryu, S. H. Kim, H. G. Park, J. K. Hwang, Y. H. Lee, and J. S. Kim, "Square lattice photonic bandgap single-cell laser operating in the lowest-order whispering gallery mode," *Appl. Phys. Lett.*, vol. 80, pp. 3883–3885, 2002.
- [6] C. Monat, C. Seassal, X. Letartre, P. Regreny, P. Rojo-Romeo, P. Viktorovitch, M. L. V. d'Yerville, D. Cassagne, J. P. Albert, E. Jalaguier, S. Pocus, and B. Aspar, "Modal analysis and engineering on InP-based two-dimensional photonic-crystal microlasers on a Si wafer," *IEEE J. Quantum Electron.*, vol. 39, no. 3, pp. 419–425, Mar. 2003.
- [7] J. R. Cao, W. Kuang, Z.-J. Wei, S. J. Choi, H. Yu, M. Bagheri, J. D. O'Brien, and P. D. Dapkus, "Sapphire-bonded photonic crystal microcavity lasers and their far-field radiation patterns," *IEEE Photon. Technol. Lett.*, vol. 17, no. 1, pp. 4–6, Jan. 2005.
- [8] G. V. Samsonov, *The Oxide Handbook*, 2nd ed. New York:IFI/Plenum, 1982.
- [9] L. A. Coldren and S. W. Corzine, *Diode Lasers and Photonic Integrate Circuits*. New York: Wiley, 1995.
- [10] A. Mathur and P. D. Dapkus, "Fabrication, characterization and analysis of low threshold current density 1.55- μm -strained quantum-well lasers," *IEEE J. Quantum Electron.*, vol. 32, no. 2, pp. 222–226, Feb. 1996.
- [11] A. Yariv and P. Yeh, *Optical Waves in Crystals*. New York: Wiley, 1983.
- [12] O. Painter, J. Vuckovic, and A. Scherer, "Defect modes of a two-dimensional photonic crystal in an optically thin dielectric slab," *J. Opt. Soc. Amer. B*, vol. 16, pp. 275–285, 1999.
- [13] C. W. Kim, W. J. Kim, A. Stapleton, J. R. Cao, J. D. O'Brien, and P. D. Dapkus, "Quality factors in single-defect photonic-crystal lasers with asymmetric cladding layers," *J. Opt. Soc. Amer. B*, vol. 16, pp. 1777–1781, 2002.